Simulation and performance of Pulsed Pipe Flow Mixing in Non-Newtonian Liquid Dispersion Media

T. Koiranen[*1], J. Tamminen[1], and A. Häkkinen[1]
[1] LUT Chemtech, Lappeenranta University of Technology, Lappeenranta, Finland
*Corresponding author: LUT, P.O. BOX 20, F-53851, Lappeenranta, Finland, tuomas.koiranen@lut.fi

Abstract: A non-newtonian water based oil dispersion in a pulsed flow pipe system was mixed in a circulation loop pipe with custom-made static mixers and empty tubes at different flow rates. The rotor-pump was used in a non-pulsed flow circulation, and diaphragm pump for pulsed flow circulation. Comsol Multiphysics 4.3b was used for the modeling and simulation. The simulations were performed using single-phase laminar flow model in steady-state and in time-dependent modes based on the pump type. The pulsed flow was modeled using the sinusoidal form of velocity inlet boundary condition. The mixing was modeled using diluted species transport equation. The simulation was used for the estimation of the fluid mixing efficiencies of pulsed and non-pulsed flows based on the coefficient of variation CoV. Pulsed flow did not improve mixing in a circulation pipe loop. The flow simulations assured also experimentally observed high pressure peaks when pulsed flow diaphragm pump is used.

Keywords: Pulsatile flow, non-newtonian rheology, flow simulation

1. Introduction

Pulsating pipe flow has been studied less than constant pipe flow rate, non-pulsing flow. While pulsed pipe flow has been the subject of relatively few studies, applications of pulsed flow have been in use as pulsed liquid-liquid extraction columns. Bujalski et al. (2005) and Amokrane et al. (2014) have used Computational Fluid Dynamics (CFD) modeling in the solvent extraction pulsed column. Bujalski et al. used 2-D computational grid using single-phase low Reynolds number k-ε turbulent modeling. Amokrane et al. (2014) have studied different turbulent models in order to capture temporal velocity fields in turbulent flows. Carpinlioglu and Gundogdu (2001) have reviewed pulsed pipe flow studies. They listed several research topics that are not yet studied. These are for example transitional pulsatile flow ranges, pressure drop and velocity studies in the entrance length of laminar pulsatile flows, and also turbulence generation. Timité et al. (2010) considered laminar flow model in their CFD simulations when Re-number was below 1200. According to Yilmaz and Gungdogdu (2010) and Carpinlioglu and Gundogdu (2001) the change from laminar flow to turbulent flow should be evaluated based on the Womersley number ($\sqrt{\omega'}$) in the case of pulsating flow. The conservative start of the transition flow range is based on time-averaged of the cross-sectional mean velocity Reynolds number (Re_{ta}) at 2100.

Computational fluid dynamics (CFD) models in pulsating flows have been investigated especially in pulsatile blood flows by Vignon-Clementel et al. (2010), Jung et al. (2006) and Steinman (2002).Vignon-Clementel et al. studied flow and pressure variations due to naturally varying heart rate and noticed the sensitivity to inlet conditions for the results. Jung et al. modeled shear-thinning viscosity with Carreau-Yasada viscosity model in multiphase 3-D CFD simulation. The use of the non-newtonian viscosity model was justified based on the blood rheology and flow conditions.

According to Swamee and Aggrawal (2011), the friction factor for the laminar flow of Bingham plastic fluid is given by the Buckingham-Reiner equation, which they present also in implicit form. There is no abrupt transition from laminar to turbulent flow for Bingham plastic fluid, as the flow transforms gradually from laminar to fully turbulent. However, there is a lower critical Reynolds (Re_c) number, below which all disturbances are damped.

In this study it is shown that pulsed flow does not improve mixing when using static mixers in a circulation pipe loop. The flow simulations assured also high pressure peaks when diaphragm pump is used.

2. Governing equations

The Bingham plastic rheology of the liquid dispersion viscosity is:

$$\mu = \mu_0 + \frac{b}{\gamma} \quad (1)$$

The liquid dispersion density is:

$$\rho = w_H \rho_H + (1 - w_H)\rho_L \quad (2)$$

Time-dependent laminar flow model is:

$$\rho \frac{\partial u}{\partial t} + \rho(u \cdot \nabla)u = \nabla[-p + \mu(\nabla u + (\nabla u)^T)] \quad (3)$$

$$\rho \nabla \cdot u = 0 \quad (4)$$

The boundary condition at the inlet velocity was a smoothed triangle shaped waveform function with amplitude 0.2 and the angular frequency 12.57. The pressure boundary condition ($p = 0$) was used for the outlet.

The dilute chemical species transport model is:

$$\nabla \cdot (-D\nabla c) + u \cdot \nabla c = 0 \quad (5)$$

The boundary condition for the tracer fluid step function is:

$$c(t) = \begin{cases} 0, t < 0 \\ c(x), t > 0 \end{cases} \quad (6)$$

$$c(x) = \begin{cases} 0, x < R \\ 1, x > R \end{cases} \quad (7)$$

The experimental and simulated mixing efficiencies are compared based on the coefficient of variation:

$$CoV = \frac{\sigma}{X_{average}} \quad (8)$$

The mixing is the most efficient when CoV-value approaches to 0.

Mixing power of static mixers is calculated:

$$P = \Delta p Q \quad (9)$$

3. Experimental

Mixing experiments were made in a 50 L mixing tank and a circulation loop (Fig. 1). The circulation loop consisted of a steel tube (length = 1.7 m), which was equipped with two static mixers and three pressure sensors (Wika S-11) (see Fig. 1). The inner diameter of the tube was 0.030 m. For comparison purposes, the static mixer elements were replaced with straight tubes of same inner dimensions. Two pumps, a non-pulsing rotor pump (Zuwa Nirostar A) 17 L/min and a pulsed flow diaphragm pump (Sandpiper EB) 22 - 30 L/min with 0.8-2.3 Hz operating frequency were used to circulate the fluids in the loop. The amplitude of the diaphragm pump was for example 8.5 L/min at 27.6 L/min. The amplitude of the inlet velocity was determined based on video data and volumetric flow measurements from the outlet. The frequency was determined based on the recorded sound track of the diaphragm pump. The static mixer was original design by LUT Chemtech, and simple geometry was one of design criteria (see Fig. 2).

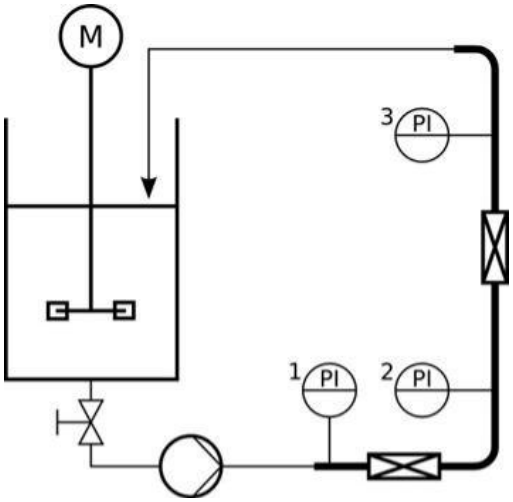

Figure 1. Experimental set-up of the mixing tank and the circulation loop. The numbering of pressure meters is shown. Thick line indicates steel tube, where static mixers and pressure meters are installed.

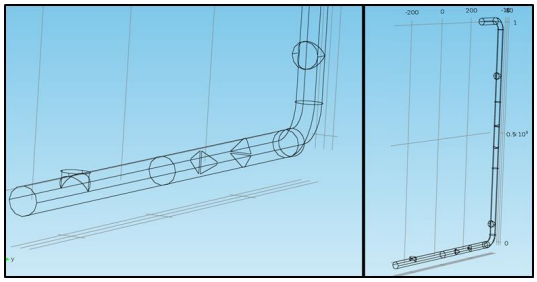

Figure 2. Static mixer configuration, and static mixer-loop geometry modeled with COMSOL Multiphysics.

The feed solution was water containing oil, which comprised immiscible heavy and light liquid phases. Compositions can change, but they typically consist of mixture of water and organic compounds such as aldehydes, carboxyacids, carbohydrates and polymerized aromatic alcohols. Densities of light phase, heavy phase and dispersion were 1.16 g/mL, 1.21 g/mL and 1.17 g/mL, respectively. The mass fractions of the light and heavy phases were 0.8 and 0.2, respectively. The mixture was studied with an Anton-Paar Modular Compact Rheometer MCR 302. The behavior of the mixed dispersion was Bingham plastic (Fig. 3). The fluid viscosity is constant 30 mPas at the measurement range 25-100 1/s.

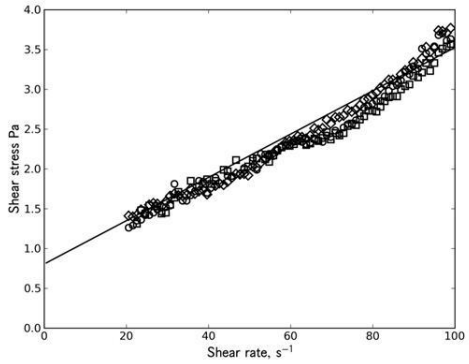

Figure 3. Measurement data for the biobased water-oil dispersion rheology. Data from three parallel measurements with a rheometer (Anton Paar MCR 302) are shown. The measurements were made at 25 °C.

The monitoring of the mixing was as follows. The samples were taken in the mixing tank between 10 and 60 minutes after the experiment was started. The heavy and the light phases were separated by ultracentrifugation from the samples, and mixing was calculated based on the heavy phase mass fraction in the sample X_R. The deviation of the heavy phase weight fraction in the samples was used to describe the mixing efficiency based on the Eq. (8). The mixing of the liquid dispersion is typically stronger as the phase separation is slower. This implies that heavy phase will settle slower in the mixing tank, and the heavy phase mass fraction is kept constant. Therefore the deviation in the well-mixed experiments is small, and the average heavy phase mass fraction in the sample is high. When straight tube elements were installed into circulation loop, obvious decrease in mass fraction of heavy phase could not be observed. It was based on the samples when circulation experiment was continued from 30 to 60 minutes. This indicated that dispersion did not settle in the mixing tank.

4. Methods

A CFD model using Comsol Multiphysics 4.3b (COMSOL Multiphysics® 4.3 Reference Guide, 2013) was made for the static mixer elements in the mixing loop that was used in the actual measurements (Fig. 2). The modeling was done for non-pulsed flow 17 L/min (flow velocity 0.4 m/s) and pulsed flow 27.6±8.5 L/min (0.65±0.2 m/s). The non-pulsed flow simulation corresponds to the use of the rotor pump and the pulsed flow corresponds to the diaphragm flow. The average shear rate (Severs and Austin, 1954) was between 110 1/s and 230 1/s in the given flow conditions. Constant viscosity 30 mPas was estimated on the basis of the measurement data (Fig. 3) to describe Bingham plastic rheology in the simulations. The Reynolds number in the case of constant flow 17 L/min was 468, and in the pulsed flow 527 - 995. According to the Reynolds number the flow is at laminar flow region. The Womersley number was 10.5. The Womersley number greater than 1.32 indicates on the other hand the creeping transition flow (Carpinlioglu and Gundogdu, 2001). In the modeling the laminar flow model was decided to be used as Timité et al. [2010] did with the same magnitude Reynolds number region.

The present studies were done using single phase flow simulations and using the chemical species transport model. The non-pulsed flow was simulated as a steady-state simulation. The pulsed flow was simulated as time-dependent solution with an adaptive time-step. The simulation time in this case was selected greater than the time of fluid flow in tube. The flow velocity boundary condition was used for the inlet and the pressure boundary condition was used in the outlet. The calculations were accomplished in an unstructured grid of 206008 elements. Average cell volume used in simulations was 5.8 µL as tube volume was 1.25 L. Constant viscosity was used because of the measured fluid rheology data, and that the average shear rate values were as high as 110-

230 1/s. It is however noticed that the shear rate at walls approach 0 1/s, as no-slip condition was used. Crosswind and streamline diffusion schemes were used in the transport of diluted species model for the modeling of the tracer fluid test. Diffusion coefficient was 10^{-9} m^2/s which minimizes the diffusive transport effect. The tracer fluid test was performed as a time-dependent simulation. The calculated pressures were obtained from the corresponding measurement positions 1, 2 and 3 as shown in Fig. 1.

5. Experimental results

Pressure data was recorded in all circulation experiments. In the case of pulsed flow circulation experiments, the readings of the pressure meters varied rapidly alongside the flow. Estimates for pressure drop in the pulsed flow experiment are presented in Table 1, and they have great uncertainties. In the case of non-pulsed flow, the measured pressure drop data did not have any variation.

The mixing power of the tube/static mixer elements was calculated from Eq. (9). The mixing power in the circulation loop was then compared to the CoV values (Fig. 4).

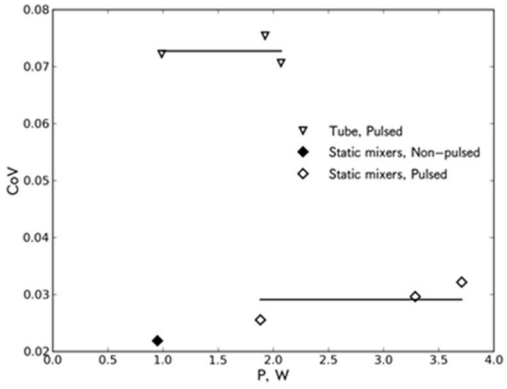

Figure 4. Coefficient of variation (CoV) to the measured mixing power of two static mixer/tube elements. The lines indicate the average value of CoV.

Table 1: Pressure drop estimates and mixing power for static mixers and without static mixers. Values for pulsed flow experiments are averages of measured pressure drops.

Static mixers Pulsed flow		
Q, L/min	Δp_{tot}, Pa	P_{tot}, W
23	5000±1500	1.9±0.6
28	6900±1500	3.2±0.7
29	7700±1500	3.7±0.7
Static mixers Non-pulsed flow		
17.3	3300±50	1.0±0.1
Tube Pulsed flow		
22	2700±1500	1.0±0.6
28.4	4000±1500	1.9±0.7
29.6	4200±1500	2.1±0.7
Tube Non-pulsed flow		
17	500±50	0.1±0.1

6. Simulation results

The simulated pressure difference between positions 1 and 3 was 3800 Pa and the measured pressure was 3300 Pa in the case of non-pulsed flow at constant flow velocity 0.4 m/s. In the case of pulsed flow the average simulated pressure difference between positions 1 and 3 was 7600 Pa, and the average measured pressure was estimated 6900±1500 Pa at flow velocity 0.65±0.2 m/s. The maximum simulated pressure differences in pressure meters 1, 2 and 3 were 15600 Pa, 9100 Pa and 2000 Pa, see Fig. 5. The flow velocity and pressure profiles for the pulsed flow simulation are presented in Fig. 6. The calculated mixing power from simulation results for non-pulsed flow (0.4 m/s) was 1.1 W. The calculated mixing power for pulsed flow (0.65±0.2 m/s) from simulation was 3.5 W. According to the simulation results the non-pulsed flow with considerably smaller mixing power leads to better mixing than the pulsed flow.

The CoV was simulated using a step function and the chemical species transport equation. The concentration step (Eqs. 6 and 7) was set just before the first static mixer, and the response was read just before the first 90° pipe curve. The average concentration and the standard deviation

were calculated based on the cross-sectional plane of the pipe by taking area-weighted concentration values according to Hirschberg et al. (2009). The simulated CoV for one static mixer in the case of the non-pulsed flow at 0.4 m/s was 0.23. In the case of the pulsed flow at 0.65±0.2 m/s it was 0.25, see Fig. 7.

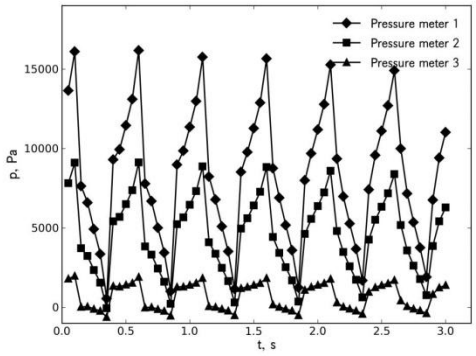

Figure 5. Simulated pressure curves for laminar pulsed flow in static mixer loop.

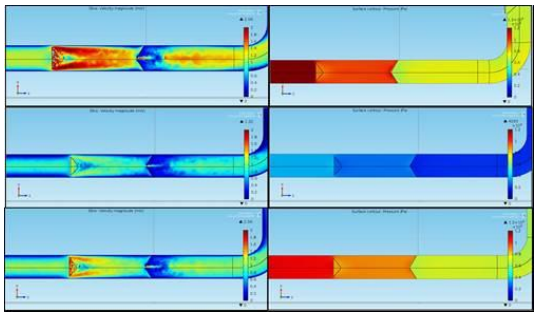

Figure 6. Flow velocity (m/s) profile (left) and pressure (Pa) profile (right) in the first static mixer at times t = 0.125 s (figure above), 0.375 s (middle) and 0.5 s (figure below).

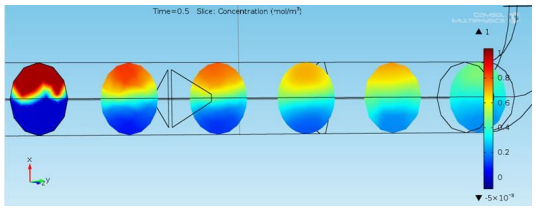

Figure 7. Visualization of the concentration step function throughout the first static mixer introduced at time step 0.5 s, the average flow velocity is 0.65 m/s. The distance between the isosurfaces is 67.8 mm.

7. Discussion

The difference in the measured and simulated pressure drops was about 500 Pa. This may be due to the small errors in the geometry model compared to the real geometry. Pressure drops and thus the mixing power measured for dispersion mixing with the static mixer were compared to those presented in the literature (Thakur et al., 2003). The mixing power from their correlations especially for the Sulzer SMX (0.5 W - 2 W) and Sulzer SMV (1.5 W - 4.7 W) were of the same order of magnitude as those present in the static mixer used in this study. The great advantage in the CFD simulations was that the pulsed flow pressure variations could be explained by the nature of the pulsed flow.

The numerical comparison of the CoV-values between the measurements and the simulations is not valid because the simulations were concentrated for the mixing of one static mixer element, and the CoV calculation was based on the positional concentration differences. On the other hand the measured CoV was based on the time dependent sampling. The both simulated and experimental results indicate however the same trend that the non-pulsed flow seemed to lead to better mixing than the pulsed flow. It is emphasized here that the mixing in non-pulsed flow is even better with 70 % smaller mixing power. According to Pahl and Muschelknautz (1982), a similar result is achieved when very high liquid velocities are used in emulsification with a static mixer. The liquid flow becomes pulsed, which hinders further emulsion formation.

8. Conclusions

The water-oil solution, which consisted of immiscible heavy and light liquid phases, was mixed in novel static mixers. The solution was mixed with static mixers installed in a circulation loop. CFD simulations revealed high pressure variations at individual pressure meters, which were at first observed in the measurements. The efficiency of the static mixing in the dispersing immiscible liquids was studied based on the CoV-values. The both simulated and experimental results indicate the same trend that the non-pulsed flow leads to better mixing than the pulsed flow.

9. Symbols

b	Constant, -
c	Concentration, -
d	Pipe diameter, m
f	Frequency, Hz
P	Mixing power, W
p	Pressure, Pa
R	Pipe radius, m
Q	Volumetric flow rate, L/min
t	Time, s
V	Volume, L
u	Flow velocity, m/s
w_H	Heavy phase mass fraction in dispersion, -
x	Position, m
$X_{average}$	Average of the heavy phase mass fraction samples, -

Greek alphabet

Δp	Pressure drop, Pa
γ	Shear rate, 1/s
μ	Dispersion dynamic viscosity, Pas
μ_0	Dispersion dynamic viscosity, Pas
ρ	Liquid dispersion density, kg/m^3
ρ_H	Density of the heavy phase, kg/m^3
ρ_L	Density of the light phase, kg/m^3
σ	Standard deviation, -

Abbreviations

$Re=\rho ud/\mu$	Reynolds number for pipe flow
CoV	Coefficient of variation
$\sqrt{\omega'}=R(2\pi f)^{½}$	Womersley number

10. References

1. Amokrane A., Charton, S., Lamadie F., Paisant J.F., Puel, F., Single-phase flow in a pulsed column: Particle Image Velocimetry Validation of a CFD based model, *Chemical Engineering Science*, **114**, 40-50 (2014).

2. Bujalski, J.M., Yang, W., Nikolov, J., Solnordal, C.B., Schwarz, M.P., Measurement and CFD simulation of single-phase flow in solvent extraction pulsed column, *Chemical Engineering Science*, **61**, 2930-2938 (2006).

3. Carpinlioglu, M.O., Gundogdu, M.Y., A critical review on pulsatile pipe flow studies directing towards future research topics. *Flow Measurement and Instrumentation*, **12**, 163–174 (2001)

4. Hirschberg, S.; Koubek, R.; Moser, F.; Schöck, J. An improvement of the Sulzer SMX static mixer significantly reducing the pressure drop. *Chemical Engineering Research and Design*, **87**, 534–532 (2009).

5. Jung, J., Lyczkowski, R.W., Panchal, C.B., Hassanein, A., Multiphase hemodynamic simulation with pulsatile flow in a coronary artery, *Journal of Biomechanics*, **39**, 2064-2073 (2006).

6. Pahl, M. H.; Muschelknautz, E. Static mixers and their applications. *International Chemical Engineering*, **22**, 197–205 (1982).

7. Severs, E. T.; Austin, J. M. Flow properties of vinyl chloride resin plastisols. *Ind. Eng. Chem.*, **46**, 2369–2375 (1954)

8. Steinman, D.A., Image-based computational fluid dynamics modeling in realistic arterial geometries, *Annals of Biomedical Engineering*, **30**, 483-497 (2002).

9. Swamee, P.K.; Aggarwal, N. Explicit equations for laminar flow of Bingham plastic fluids. *Journal of Petroleum Science and Engineering*, **76**, 178–184 (2011).

10. Thakur, R. K.; Vial, Ch.; Nigam, K. D. P.; Nauman E. B.; Djelveh, G. Static mixers in the process industries – A review. *Trans IChemE*, **81A**, 787–823 (2003).

11. Timité, B.; Castelain, C.; Peerhossaini, H. Pulsatile viscous flow in a curved pipe: effects of pulsation on the development of the secondary flow. *International Journal of Heat Fluid Flow*, **31**, 879–896 (2010).

12. Vignon-Clementel, E., Figueroa, C.A., Jansen, K.E., Taylor, C.A. Outflow boundary conditions for three-dimensional simulations of non-periodic blood flow and pressure fields in deformable arteries, *Computer Methods in Biomechanics and Biomedical Engineering*, **13**, 625-640 (2010)

13. Yilmaz, F., Gundogdu, M.Y., Experimental and Computational Investigation of Velocity Field for Intermediate Region of Laminar Pulsatile Pipe Flow, *Journal of Thermal Science and Technology*, **30**, 21-35 (2010).